

Student: Alejandro Lecinas, MSII | The University of Arizona College of Medicine – Tucson

OLFACTOMEDIN-1 ACTIVITY IDENTIFIES A CELL INVASION CHECKPOINT DURING EPITHELIAL-MESENCHYMAL TRANSITION IN THE EMBRYONIC HEART.

Alejandro Lecinas^{1,2}, Danny C. Chhun¹, Kelvin P. Dan^{1,3}, Kristen D. Ross¹, Elizabeth A. Hoover¹, Parker B. Antin¹ and Raymond B. Runyan¹

Departments of Cellular and Molecular Medicine¹
Pharmacology and Toxicology² and Program in Physiological Sciences³.
The University of Arizona, Tucson Arizona 85724.

This article was previously published in *Disease Models & Mechanisms*.

SUMMARY:

Endothelia in the atrioventricular (AV) canal of the developing heart undergo a prototypical epithelial mesenchymal transition (EMT) to begin heart valve formation. Using an *in vitro* invasion assay, an extracellular matrix protein found in the heart, Olfactomedin-1 (OLFM1), increases mesenchymal cell numbers. Both anti-OLFM1 antibody and OLFM1 siRNA treatment inhibit mesenchymal cell formation. OLFM1 does not alter cell proliferation, migration or apoptosis. Dispersion, but lack of invasion in the presence of inhibiting antibody, identifies a specific role for OLFM1 in cell invasion during EMT. This role is conserved in other epithelia, as OLFM1 similarly enhances invasion by MDCK epithelial cells in a trans-well assay. OLFM-1 activity is cooperative with TGFβ, as synergy is observed when TGFβ2 and OLFM1 are added to MDCK cell cultures. Inhibition of both OLFM1 and TGFβ in heart invasion assays shows a similar cooperative role during development. To explore OLFM1 activity during EMT, representative EMT markers were examined. Effects of OLFM1 protein and anti-OLFM1 on transcripts of cell-cell adhesion molecules and the transcription factors, *Snail-1*, *Snail-2*, *Twist1*, and *Sox-9*, argue that OLFM1 does not initiate EMT. Rather, regulation of transcripts of *Zeb1* and *Zeb2*, secreted proteases and mesenchymal cell markers by both OLFM1 and anti-OLFM1 is consistent with regulation of the cell invasion step of EMT. We conclude that OLFM1 is present and necessary during EMT in the embryonic heart. Its role in cell invasion and mesenchymal cell gene regulation suggests an invasion checkpoint in EMT where OLFM1 acts to promote cell invasion into the three-dimensional matrix.

INTRODUCTION:

Epithelial Mesenchymal Transition (EMT) is a cellular process that mediates transition from two-dimensional cellular sheets to a three-dimensional structure (Hay, 1995). EMT is widely utilized by the embryo for gastrulation, neural crest cell formation, heart valve formation and other developmental processes (Hay, 1995; Yang and Weinberg, 2008). In the adult, EMTs occur in the pathologies of both metastasis and organ fibrosis (Thiery et al., 2009). EMT is initiated through a variety of signals including growth factors, inflammatory signals and extracellular proteases (Thiery et al., 2009; Nieto, 2011). A common view is that induction or stabilization of one or more transcriptional repressors such as SNA1 or ZEB1 leads to loss of cell-cell adhesion and initiates a cascade of processes leading to EMT (Nieto, 2011). The details of this cascade are still being explored but its interruption may lead to epithelial plasticity or a metastable state rather than a complete transition (Klymkowsky and Savagner, 2009). In avian heart valve formation, EMT is mediated by activities of TGFβ2 and TGFβ3, but sequential regulation has not been identified in any other EMT (Boyer et al., 1999). We identify here a novel regulator of cell invasion during EMT in the avian heart, olfactomedin-1 (OLFM1). These findings extend the observation that EMT is mediated by sequential signals and that the ability of a cell to invade a matrix is a regulated element of EMT.

OLFM1 (variant 1) (also known as Noelin-1 and Pancortin-1) is an extracellular matrix protein expressed in the developing heart (reported here), the central nervous system and in a variety of tumor tissues (Moreno and Bronner-Fraser, 2005; Sun et al., 2006; Kim et al., 2010). It is a member of the olfactomedin family of proteins and contains a conserved 250 amino acid olfactomedin domain. Olfactomedin domains are binding sites for protein-protein interaction between olfactomedin family members such as Myocilin and Olfactomedin-3 (Tomarev and Nakaya, 2009). There are four numbered variants of OLFM 1 with variant 1 as the longest isoform (Barembaum et al., 2000). Though called Noelin-1 in the avian species, we use OLFM1 here as the conserved gene name. Avian OLFM1 is conserved across species with 92% amino acid sequence similarity with *Xenopus* and 85% similarity to murine OLFM1. Mouse and chick transcripts have numbered isoforms, 1-4, generated through alternative splicing. The nomenclature in the human is different as OLFM1 is a homolog of No-

elin-1 and Pancortin-1 but human Olfactomedins 2-4 are unique gene products. Alternately spliced forms of OLFM1 in humans are referred to as variants 1-4.

OLFM1 was found to induce additional neural crest cells in the embryo (Barembaum et al., 2000), a process that includes EMT as well as cell differentiation and migration. As its role in neural crest formation was undefined, we examined OLFM1 during formation of valves in the embryonic chick heart. EMT in the heart is a well-described process based on *in vitro* analysis by a collagen gel assay (Potts and Runyan, 1989; Brown et al., 1996; Boyer et al., 1999; Tavares, 2006). The EMT assay recapitulates the formation of AV valve progenitors from endothelial precursors (Markwald et al., 1977; Potts and Runyan, 1989; Boyer et al., 1999; Yang and Weinberg, 2008).

Immunostaining confirmed synthesis of OLFM1 protein by the myocardium. OLFM1 is an extracellular matrix molecule and may be a component of the tissue interaction in the heart (Barembaum et al., 2000; Moreno and Bronner-Fraser, 2002). Mesenchymal cells are derived from cardiac endothelium in EMT induced by the myocardium (Markwald et al., 1984). Exogenous OLFM1 increased mesenchymal cell numbers and anti-OLFM1 inhibited mesenchyme formation from cardiac explants in the collagen gel assay. Anti-OLFM1 had no effect on endothelial cell separation that identifies the initiation of EMT, but inhibited subsequent invasion of activated endothelial cells. Confirmation of the activity of OLFM1 was shown by similar siRNA perturbation of mesenchyme. OLFM1 is auto-regulatory as addition of OLFM1 to explanted cultures induces expression of *OLFM1* mRNA. To examine effects of OLFM1 on mammalian cells, MDCK epithelial cells were placed in a trans-well invasion assay with TGFβ2, OLFM1 or a combination of the two factors. We found TGFβ2 and OLFM1 to be synergistic in mediating cell invasion. The combination of OLFM1 siRNA and anti-TGFβ showed a similar inhibition of EMT in heart explant cultures. These extracellular factors appear to work in concert to promote cell invasion.

These results define OLFM1 as a regulator of invasion in EMT. This suggests that initiation of cell invasion is a discrete checkpoint in the EMT process where OLFM1, TGFβ and, perhaps other signals, mediate the transition from activation to invasion. The existence of an invasion

checkpoint is consistent with both previous observations with the neural crest and the concept of epithelial plasticity, where an incomplete EMT is observed (Barembaum et al., 2000; Thiery et al., 2009). As OLFM1 is conserved across species and it is expressed in a number of tumors, its role in invasion during EMT is likely to extend to a widespread role in both normal developmental and adult pathology.

RESULTS:

OLFM1 is produced by the myocardium in the embryonic heart

Preliminary PCR analysis established that *OLFM1* mRNA was expressed in the heart (not shown). To identify the source of OLFM1 in the heart, embryo sections (stage 15 HH) were stained with a commercial antibody for OLFM1 and counterstained with a cardiac myosin marker, MF-20, and a nuclear marker, DAPI. Though the antigen for antibody production was mouse recombinant OLFM1 protein, the antibody identified a predominant band of approximately 50kD in chicken tissue, similar to that previously reported by Barembaum et. al. (2000) (Supplemental Figure 1).

OLFM1 staining was observed in the myocardium while the endothelium was unstained (Fig. 1). The figure shows the heart in cross-section through the outflow tract and through a portion of the heart that includes the atrioventricular (AV) canal and common ventricle. The most intense staining was observed in the AV canal portion of the myocardium. OLFM1 was not present in the mesenchyme of the head or in adjacent thoracic tissue. At higher magnification (Fig. 1C), staining was more intense on the endocardial side of the myocardium, the portion of the myocardium that is the site of secretion of cardiac extracellular matrix (ECM) (Kitten et al., 1987). As the inductive stimulus for EMT is derived from the myocardium (Krug et al., 1985; Kitten et al., 1987), this distribution is consistent with OLFM1 as a component of the tissue interaction. OLFM1 expression was also seen in mesenchymal cells of the AV canal after EMT (arrows, Figure 1D)

OLFM1 regulates mesenchymal cell formation in the heart

OLFM1 was examined in an established assay for embryonic EMT (Runyan and Markwald, 1983). An initial dose-response assay surveyed two markers of mesenchymal cell formation, Fibulin2 (FBLN2) and aldehyde dehydrogenase 1a1 (ALDH1A1) with AV explants (Supplemental Figure 2). Fibulin2 is a well-established marker of EMT in the heart synthesized by newly formed mesenchyme (Wunsch et al., 1994). ALDH1A1 is a stem cell marker (Ginestier et al., 2007) and a useful measure of mesenchymal cell formation in explant cultures (Supplemental

Figure 3) as the expression of stage 14 chick embryo peaks at 36 hours after dissection and declines after differentiation from mesenchymal cells at 48 hours. Stage 15 AV canal explants were treated with 0, 100, 200, 300 and 400 ng/ml of mouse recombinant OLFM1 for 36 hours and the marker expression was assessed by real time RT-PCR. The dose response curve was bell-shaped with the largest response seen at the 200 ng/ml for both markers (Supplemental Figure 4). We found OLFM1 mRNA in heart explants to be regulated by exogenous OLFM1 in a pattern that replicated the mesenchymal markers (Fig. 2a). This suggests that OLFM1 is auto-regulatory. In additional experiments (below) we treated MDCK epithelial cells with OLFM1 to examine its effects on a mammalian epithelium. ALDH1a1 and FBLN2 proved to be poor markers for EMT in MDCK cells but OLFM1 mRNA was up-regulated by OLFM1 protein in these cells. The dose response to OLFM1 was measured by production of OLFM1 mRNA after 24 hr exposure. The data showed a plateau beginning at 200 ng/ml (Fig. 2b). The difference in response may reflect differences between a developing tissue and a cell line but the 200 ng/ml dose appeared to be useful for both primary explants and the MDCK cell line.

To assess effects of OLFM1 on endothelial cells, Stage 15 (Hamburger and Hamilton, 1951) AV canal explants were cultured on a collagen gels with either exogenous OLFM1 (200 ng/mL) or anti-OLFM1 (10 µg/mL) antibody for 36 hours. Cultures were fixed and photographed to examine morphology and to quantify mesenchymal cells. Control cultures displayed activated endothelial cells dispersed on the gel surface (Fig. 3a) while mesenchymal cells were observed within the gel matrix using Hoffman Contrast Optics (Fig. 3e). Cultures treated with OLFM1 displayed a similar endothelial outgrowth and a greater number of mesenchymal cells (Fig. 3b, f). Quantification showed that mesenchymal cells (20 explants/ treatment) increased 79% in explants treated with OLFM1 (Fig. 2i).

In contrast, affinity-purified anti-OLFM1 antibody inhibited mesenchymal cell formation in AV canal cultures (Figure 3g). Unlike reagents that block initial steps of EMT (Boyer et al., 1999; Mercado-Pimentel et al., 2007), antibody treatment showed normal endothelial cell separation on the cell surface (Fig. 3c). There was a decrease by 40% of mesenchymal cells, within the gel matrix, in explants treated with anti-OLFM1 antibody (Fig. 3j). Additional stage 15 AV canal explants were treated with non-specific IgG antibody as a control. The number of invaded cells in the IgG treated group did not change when compared to the untreated control (Fig 3j).

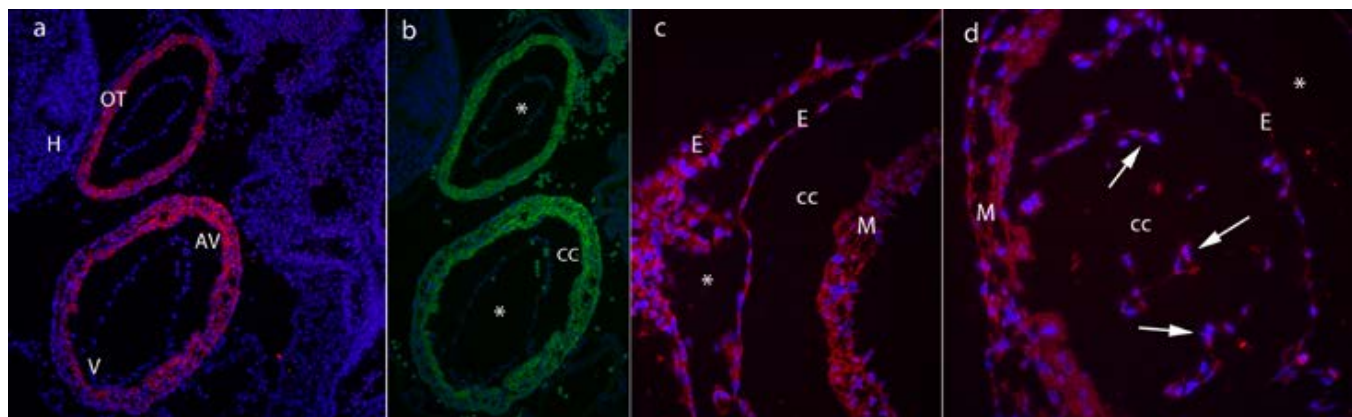


Figure 1. OLFM1 is present in myocardium of the heart just before EMT. Panel a, Stage 15 chicken AV canal immunostained for OLFM1 (Red) shows expression in the ventricle (V), atrioventricular canal (AV) and outflow tract (OT). Neighboring head (H) cells of the embryo show no protein expression of OLFM1. Panel b, shows the same section as panel a, immunostained for the myocardial cell marker, MF20. The lumen (*) and the extracellular matrix compartment (CC=cardiac cushion) intervening between the myocardium and endothelium are identified. Endothelia of the cardiac cushions in the AV canal region will undergo EMT at stage 17 by stimulus from the myocardium. Panel c, is a magnified view of an AV canal with OLFM1 expressed in the inner layers of myocardium (M) and endothelium (E). Panel d, Mesenchymal cells (arrows) show staining as well.

To confirm functional antibody specificity, exogenous mouse recombinant OLFM1 and anti-OLFM1 were added together to AV explant cultures. Anti-OLFM1 inhibited mesenchymal cell formation in the presence of exogenous OLFM-1 (Fig. 3h). Cell counts of mesenchyme showed a level of inhibition similar to antibody alone (Fig. 3k).

OLFM1 does not alter cell proliferation, death or rate of migration

Changes in mesenchymal cell numbers within the gel may result from perturbation of EMT or by loss or gain of cells within the gel by cell proliferation or death. For example, effects of a canonical Wnt in this assay can be attributed entirely to proliferation or apoptosis of mesenchyme produced by Wnt-specific reagents (Person et al., 2005a).

We examined OLFM1 effects on cell proliferation. Histone H3 staining was employed to identify proliferating cells during EMT. Stained endothelial and mesenchymal cells were counted in 20 AV canal explants to produce an index of proliferation. OLFM1 did not change this index of proliferation when compared to untreated controls (Fig. 4a).

A decreased number of mesenchymal cells with anti-OLFM1 antibody treatment may be a result of cell death. AV canals were treated with anti-OLFM1 antibody and apoptotic cells in the endothelia or mesenchyme were detected using TUNEL assay. An index of apoptotic cells with or without antibody treatment was obtained from 20 AV canal explants. Apoptosis was not significantly different between controls and treated cultures (Fig. 4b), and there was no evidence of necrotic cell debris in the cultures.

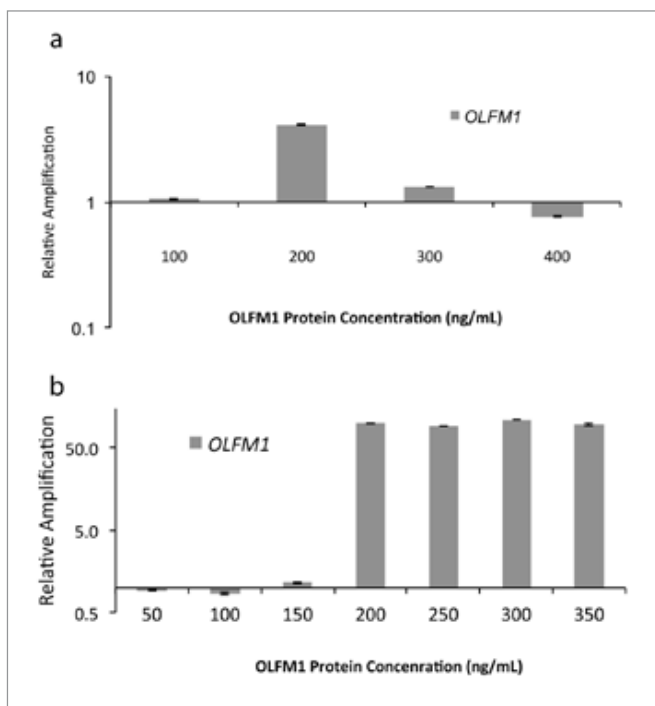


Figure 2. Dose response of avian heart tissue and MDCK cells to exogenous OLFM1 protein. Molecular responses were used to assess the dose response to exogenous OLFM1. Stage 15 AV canals were treated with various concentrations of OLFM1 Protein for 36 hours on collagen gels. Real time RT-PCR measurement showed a maximal response of mesenchymal cell markers at 200 ng/ml (Supplemental Figures 2, 3, 4). Panel 2a. Measurement of OLFM1 mRNA showed a similar up-regulation of expression at the standard 200 ng/ml dose. OLFM1 expression decreased below controls at the highest concentration (400 ng/ml). Numerical data are shown in Supplemental Table 1. Panel 2b. MDCK cells showed no expression of either ALDH1a1 or Fibulin 2 with OLFM1 treatment. The dose response to OLFM1 was evaluated by the autoregulatory expression of OLFM1 mRNA. The dose response was again maximal at 200 ng/ml but there was no inhibition at the higher doses.

An increase in mesenchymal cell numbers might be observed if mesenchymal cells migrate at a faster rate and enter the gel matrix sooner than controls. Average rates of cell migration within the gel matrix were measured. AV explants were cultured for 18 hours to produce mesenchyme within the gel. Cultures were then treated with OLFM1 (200 ng/mL) or left untreated. Beginning four hours after treatment (a time interval selected for early detectable changes in marker mRNA expression), time-lapse images were captured every three minutes using an inverted microscope with an incubator stage. Twenty individual cells were tracked for 3 hours in treated and control cultures. Image analysis (Simple PCI software) was used to produce track lengths for each cell. No significant difference in average track length between control and OLFM1 treated cells was observed (Fig. 4c).

As no differences in proliferation, cell death or migration are seen with OLFM1 or anti-OLFM1, we conclude that OLFM1 is a regulator of EMT. As there was no alteration on the initial separation (activation) of endothelium, OLFM1 is principally a regulator of cell invasion from the surface of the gel into the gel matrix.

OLFM1 induces invasion by MDCK cells

To examine whether effects of OLFM1 are specific to chick embryo endothelial cells, we tested a mammalian epithelial cell line. MDCK epithelial cells were cultured on Matrigel polymerized within trans-well inserts (8 μm pore size filter) for 24 hours with OLFM1, TGFβ2 or both factors in combination (Fig. 5). The lower surface of the filter was stained and cells that transited the gel matrix and filter were counted as epithelial cells that had undergone EMT and invaded. Cells exposed to either OLFM1 or TGFβ2 showed a small but insignificant increase in the number of invaded cells compared to untreated controls. However, there was a synergistic effect between the factors with an approximate 6-fold increase in cell invasion in the presence of both factors. A combination of OLFM1, TGFβ2 and inhibitory OLFM1 antibody showed a number of invaded cells similar to TGF2 or control treatment alone (Fig. 5).

OLFM1 siRNA Inhibits EMT

There are a number of OLFM family members that share related olfactomedin domains. Although the antibody recognizes a major protein by western blot, it may be recognizing a related family member. Similarly, the OLFM1 protein may mimic a related ligand. Examination of in situ images in the GEISHA database < http://geisha.arizona.edu/geisha/search.jsp?entrez_gene=449625 > shows only faint localization of OLFM1 in the chick heart. Of the seven OLFM-related molecules found in the chick, only OLFML2B shows a strong cardiac localization by in situ hybridization < http://geisha.arizona.edu/geisha/search.jsp?db_key_value=30973 >. We examined the expression of OLFM-related molecules in the embryonic heart by PCR. OLFM1 and 3 were present although less abundant than OLFML2B (Supplemental Figure 5). The temporal expression of OLFM1 in embryonic AV canals showed some change but was highest at stage 14 and again at stage 17 when cell invasion begins (Supplemental figure 6).

To examine specificity of OLFM1 function in the chick heart, siRNA specific for OLFM1, was incubated with stage 15 chicken AV canal explants. Explants were cultured on collagen gels to allow mesenchymal cell invasion. There was a significant decrease of mesenchymal cells (25%, p<0.05) in OLFM1 siRNA treated samples compared to scrambled controls (Fig. 6) despite the likely presence of OLFM1 protein in the explants at the time of collection. We extended this experiment to examine whether OLFM1 and TGFβ act in concert in the heart as in MDCK cells (Fig. 5). OLFM1 siRNA treated cultures were incubated with a minimal concentration of pan-TGFβ blocking antibody (1μg/ml). TGFβ antibody, at this concentration, showed inhibition of mesenchymal cells similar to OLFM siRNA alone (28%). The combination of OLFM1 siRNA and anti-TGFβ produced an additive inhibitory response consistent with the previous observation in the cell line (Fig. 6).

OLFM1 Affects a Subset of EMT Markers

EMT is an active process, characterized by transcriptional regulation of transcription factors, adhesion molecules, and secreted mesenchymal cell products. To characterize effects of OLFM1 on EMT, AV canals were treated with either OLFM1 or anti-OLFM1 antibody for 36 hours. RNA was then extracted and used to define marker gene expression changes using real time RT-PCR.

During EMT, adhesion molecule transcripts are reduced concomitant with cell separation (Nieto et al., 1994; Peinado et al., 2007; Nieto, 2011). We examined several cell-cell adhesion molecules expressed in the heart. As shown in Fig. 7a, neural cell adhesion molecule 1 (NCAM1) was unchanged with exogenous OLFM1 treatment while platelet endothelial adhesion molecule 1 (PECAM1), and cadherin-5 (CDH5) were up-regulated. Conversely, all three markers were reduced by blocking antibody. Thus, regulation by OLFM1 is inconsistent with a role in initiation of EMT. Data was graphed on a log scale to show both up- and down-regulation by the contrasting treatments. The X-axis is set at one and data are normalized to untreated controls. Supplemental Table 1 shows the numerical value and statistical significance of real time RT-PCR measurements seen in Figs. 7.

EMT is characterized by the up-regulation of several characteristic transcription factors. While specific roles are not completely understood, the zinc finger transcription factors, Snail1 or Snail2 are thought

to initiate EMT through inhibition of cell-cell adhesion transcripts (Romano and Runyan, 1999; Comijn et al., 2001; Lincoln J, 2007). *SNAI2* up-regulation is required for avian valvular EMT (Romano and Runyan, 1999). Exogenous OLFM1 increased expression of *SNAI1*, *ZEB1*, *ZEB2* and *SOX9* but reduced expression of *SNAI2* (Fig. 7b). Surprisingly, anti-OLFM1 also increased *SNAI1* and decreased *SNAI2* expression. This pattern of expression, where Snail1 and Snail2 are co-regulated by both ligand and blocking antibody, is inconsistent with early regulation of EMT but may reflect downstream regulatory interactions. OLFM1 and anti-OLFM1 produced contrasting expression of Zeb1 and Zeb2 transcripts with a strong up-regulation of Zeb2 by OLFM1. This response is consistent with the Zeb2 null mouse where neural crest cells, expressing Sox10, are induced but unable to migrate from the epithelium (Van de Putte et al., 2003). Effects of OLFM1 and its blocking antibody on Twist1 are also inconsistent with direct regulation of this molecule. Together, the regulation of these EMT transcription factors, as with the cell adhesion molecules above, is inconsistent with initiation of EMT.

EMT is accompanied by reorganization of the cytoskeleton, secretion of extracellular proteins and changes in membrane receptors (Person et al., 2005b). Although TGF- β isoforms are regulators of heart valve EMT (Boyer et al., 1999), TGF- β 2 and TGF- β 3 are also expressed by migratory mesenchyme (Boyer et al., 1999; Barnett and Desgrosellier, 2003). OLFM1 produced an increase in expression of *TGF β 3* compared

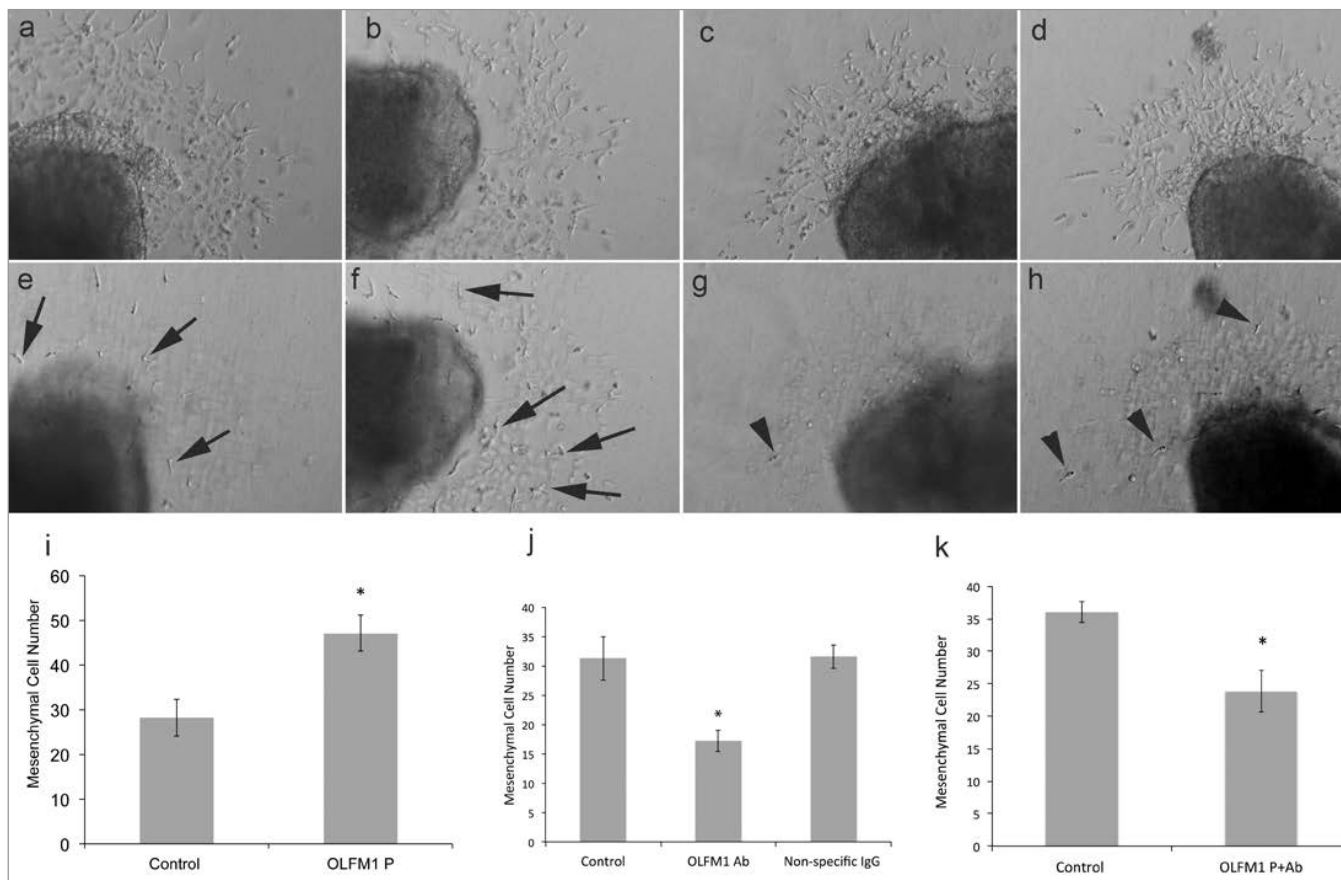


Figure 3. OLFM1 regulates EMT in the AV canal of the heart. Using the collagen assay, chicken AV canals were treated with OLFM1 protein (OLFM1 P - 200 ng/ml - Panels b & f) or OLFM1 antibody (OLFM1 Ab - 10 μ g/ml - Panels c & g) or the combination of antibody and protein (Panels d & h) for 36 hours. Panels a-d show images of AV canals on the collagen surface, while e-g show corresponding images of underlying matrix with invaded mesenchymal cells (arrows). OLFM1 P (protein) increased mesenchymal cell numbers significantly ($p \leq 0.05$, $n=20$) with OLFM1 P when compared to untreated controls (i). Mesenchymal cell counts were significantly decreased by antibody treatment compared to untreated controls or normal immunoglobulin ($p \leq 0.05$, $n=20$) (j). A combined exposure, OLFM1 P and OLFM1 Ab, confirmed that the affinity-purified antibody blocked the effects of the exogenous protein as mesenchymal cells were significantly decreased ($p \leq 0.05$, $n=20$) (k).

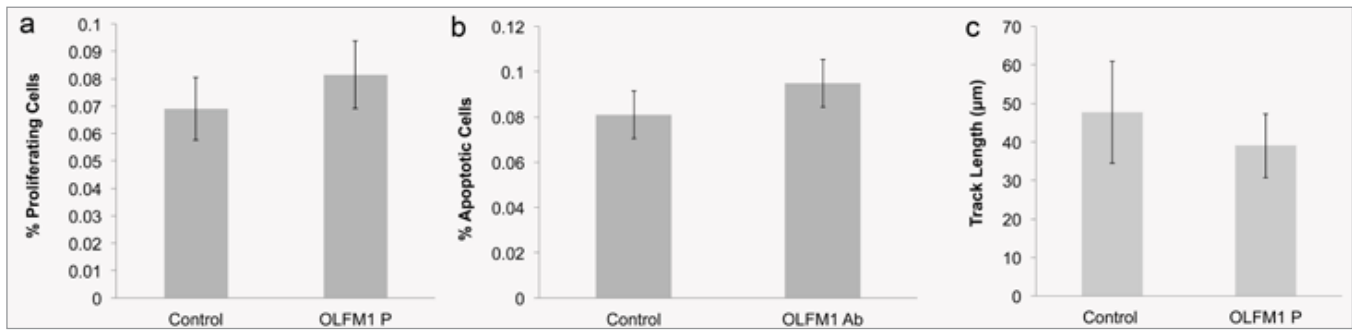


Figure 4. OLFM1 does not affect cell proliferation, cell death or cell migration. Stage 15 AV canals were treated OLFM1 protein (p) and stained for phospho-Histone-H3. The number of proliferating cells did not change significantly (n=20 explants) when compared to controls (a). Cell death after OLFM1 antibody (Ab) treatment was examined using the TUNEL assay. No significant difference (n=20 explants) in cell death was observed (b). Migration rate was determined by measuring track length of 20 individual cells every 3 minutes for 3 hr after 4 hr of OLFM1 treatment. No significant difference in track length was observed in OLFM1 treated samples when compared to untreated controls.

to untreated controls. Anti-OLFM1 decreased expression of both *TGFB2* and *TGFB3* (Fig. 7a). Fibulin-2 (*FBLN2*), and Periostin (*POSTN*), are markers of cardiac mesenchymal cells and showed both an increase in expression with exogenous OLFM1 and a corresponding decrease with anti-OLFM1. These markers reflect either a change in mesenchymal cell numbers or a change in mesenchymal cell differentiation.

VEGF receptors shift expression patterns concomitant with EMT (Stankunas et al., 2010). Vascular endothelial growth factor receptor-2 (*VEGFR2* or *FLK1*) was strongly induced with exogenous OLFM1 while *VEGFR-1* (or *FLT1*) decreased. Similarly, *ALDH1A1* expression was increased with OLFM1 addition (Fig. 5a). However, these markers were unchanged by anti-OLFM1. As the loss of mesenchyme with anti-OLFM1 (Fig. 2j) does not change baseline expression, it is likely that OLFM1 acts on activated endothelial cells (gel surface) to increase these markers as well as mesenchymal cell invasion.

Markers of both cytoskeletal reorganization (RhoA, RhoB, cofilin2 (*CFL2*) and profilin2 (*PFN2*)) and proteolytic degradation of the extracellular matrix (*PLAU*, *MMP2*, and *ADAMTS1*) were examined (Fig 5b). Small changes in *PFN2* were potentially consistent with shape change but expression of *CFL2*, *RHOA* and *RHOB* were unaffected by OLFM1 and increased with anti-OLFM1. Importantly, all three extracellular proteases tested, *PLAU*, *MMP2* and *ADAMTS1*, were strongly up-regulated by OLFM1 consistent with their roles in cell invasion.

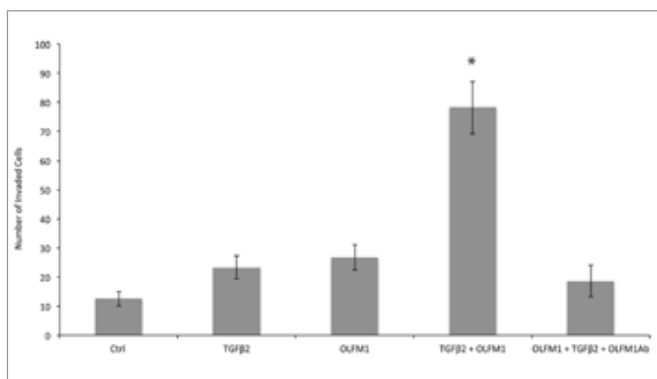


Figure 5. OLFM1 and TGFβ regulate MDCK cell invasion together. The ability of OLFM1 to stimulate cell invasion by MDCK cells was examined by a transwell assay. TGFβ2 (2ng/ml) showed a small increase in cells that transited matrigel matrix and the filter (p=0.08). OLFM1 (200 ng/ml) showed a similar increase (p=0.1). The combination of factors showed a highly significant increase in mesenchymal cells (p>0.001). OLFM1 antibody, added with both OLFM1 protein and TGFβ2, reversed the OLFM1 effect.

DISCUSSION:

The observation that OLFM1 mediates cell invasion during EMT supports the concept that there is a point during EMT in the heart when additional signals are required to enable cell invasion. In the absence of this stimulus, activated endothelial cells revert to luminal endothelia. We previously showed that EMT in the avian heart is mediated by the sequential activities of TGFβ2 and TGFβ3 and that TGFβ3 mediates invasion (Boyer et al., 1999). However, to our knowledge, this isoform switch has not been observed in any other system. The murine heart may utilize a combination of TGFβ2 and BMP but, EMT in this system happens so rapidly in vitro that, resolution of specific roles is difficult (Camenisch et al., 2002). The concept of OLFM1 driven invasion is consistent with observations on neural crest cells. Overexpression of OLFM1 produced additional neural crest cells after the first neural crest cells had left the neural tube (Barembaum et al., 2000).

Loss of either TGFβ3 (Boyer et al., 1999) or OLFM1 (this paper) leaves activated, dispersed and fusiform endothelia with limited ability to enter a three-dimensional matrix. The tumor promoting phorbol ester, PMA, produced similar activated endothelia unable to invade the gel matrix (Runyan et al., 1990). Thus, acquisition of a fusiform or dispersed phenotype is, by itself, not sufficient for cell invasion. These data suggest that there is a checkpoint where additional extracellular signals are required to enable activated cells to invade and complete

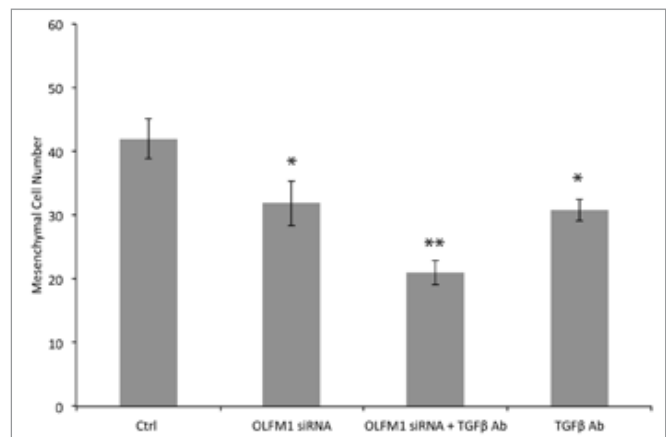


Figure 6. OLFM1 and TGFβ regulate cell invasion in the heart together. Stage 15 AV canal explants were incubated with OLFM1 siRNA, pan-TGFβ antibody or the combination of siRNA and antibody. Control and TGFβ antibody treatments included a scrambled siRNA. Both the antibody or the siRNA reduced mesenchymal cell numbers (p>0.05) and the combination reduced mesenchymal numbers still further (p>0.001)

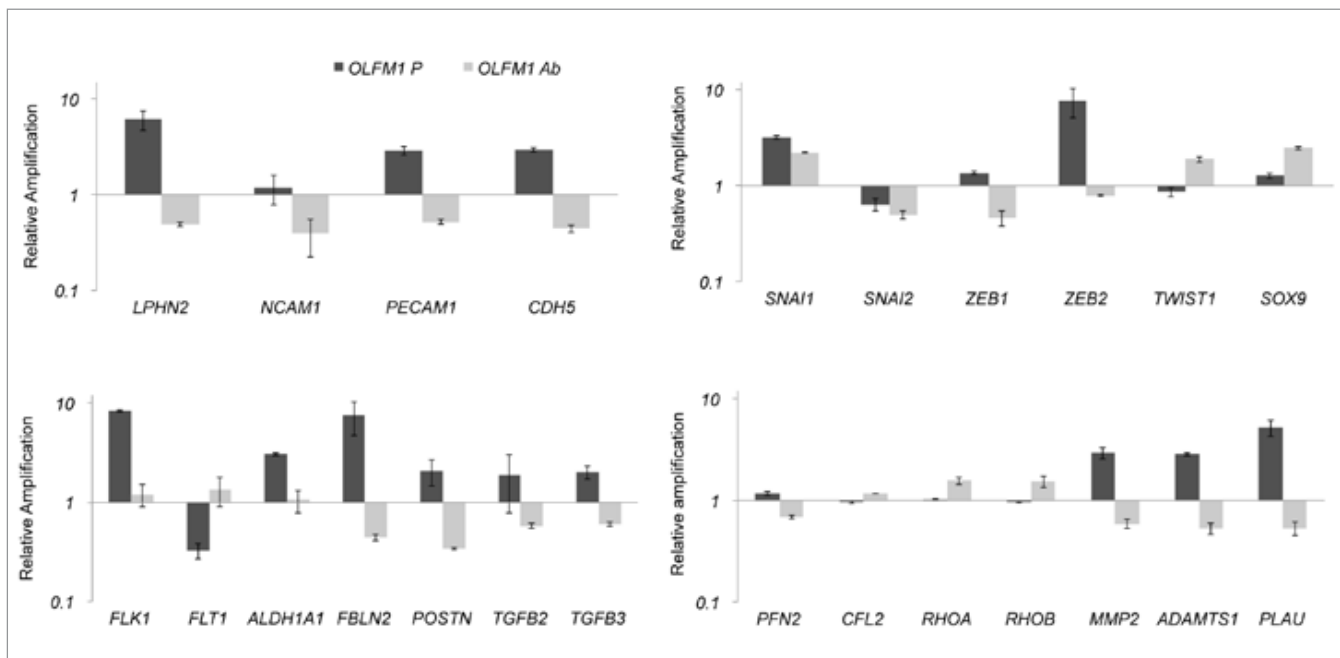


Figure 7. OLFM1 protein and antibody regulation fits late, but not early markers, of EMT. AV canals (stage 15) were treated with OLFM1 P (protein) or OLFM1 Ab (antibody) for 36 hours on the collagen gels. Real time RT-PCR expression of EMT markers was examined. Early markers included adhesion molecules (a) and transcription factors (b). **PECAM1** and **Cadherin5(CDH5)** are up-regulated by OLFM1 while **NCAM1** is unaffected. All three markers are down-regulated by the blocking antibody. **Latrophilin2 (LPHN2)** is a G protein coupled receptor that functions during late EMT. EMT-related transcription factors **Snai1**, **Snai2** and **Sox9** are either up-regulated or down-regulated by both OLFM1 and anti-OLF1. This suggests that their regulation is not related to OLFM1-mediated invasion. Mesenchymal cell products (c), actin regulators (d), and proteases (d) were investigated. Mesenchymal markers and proteases were regulated in a manner consistent with the increase or decrease of mesenchymal cells observed with OLFM1 protein or antibody activity. Cytoskeletal regulators were poorly regulated by OLFM1 reagents. Graphs use a logarithmic scale on the y-axis to show both increase and reduction from controls (1.0). Names, UID, numerical data and statistical significance are shown in Supplemental Table 1.

EMT. As OLFM1 is secreted by the myocardium, it can be viewed as a component of the inductive stimulus for EMT by the endocardium. In this light, the point at which TGFβ3 and/or OLFM1 act in the heart during EMT is a checkpoint. In the absence of either signal, the ability to invade the underlying matrix is lost or reduced.

In the present study, we employ OLFM1 protein and its corresponding antibody as contrasting treatments and controls. As shown in Fig. 3, the affinity-purified antibody specifically blocks both endogenous and exogenous OLFM1. Where the antibody and protein have contrasting effects on morphology and gene expression, we are confident of a role for OLFM1 as a regulator. In the case of three transcription EMT factors, Snai1, Snai2 and Sox9, OLFM1 protein and antibody have similar, not contrasting, effects (Fig. 7b). Though we are confident that this data is correct as it is based on three independent biological repeats, the basis for these results is unclear. We argue that this result is inconsistent with a role of OLFM1 in the initiation of EMT as Snai2 is up-regulated during EMT in the chick heart (Romano and Runyan, 1999) and down-regulated here.

Cell adhesion molecules that should be down-regulated as part of the initiation of EMT are up-regulated by OLFM1 treatment (Fig. 7a). We speculate that these data may reflect a reversion of activated cells to the endothelial phenotype. In the heart, the entire AV endocardium is activated but only about ten percent of endothelial cells complete EMT (Runyan et al., 1990). The eventual return of a majority of endothelial cells to a quiescent state has the developmental advantage of retaining luminal endothelia in the heart. This is consistent with a checkpoint where additional EMT stimulatory and inhibitory signals are received to regulate invasion.

Cancer cells with both epithelial and mesenchymal characteristics have led to the concept of epithelial plasticity or a metastable state (Derynck and Akhurst, 2007). This intermediate state during metastasis may reflect cells unable to complete EMT or delayed at a checkpoint in the absence of additional stimuli. Up-regulation of invasion markers including, proteases, ECM molecules and Zeb2 by OLFM1 is consistent with a checkpoint to regulate the final cell invasion. Other factors known to regulate proteases or matrix adhesion molecules during EMT may similarly act at invasion rather than at initiation of EMT (Yeh et al., 2006; Kessenbrock et al., 2010). As we have already seen that TGFβ3 is a component of cell invasion in the chick and TGFβ1 is recognized as a mediator of EMT (Derynck and Akhurst, 2007), we suggest that OLFM1 and TGFβ act at an invasion checkpoint during EMT.

Addition of exogenous OLFM1 increases the number of mesenchymal cells from cardiac explants. Conversely, an inhibitory antibody reduces mesenchymal cell numbers. Changes in mesenchymal cell numbers may occur through altered EMT, cell proliferation, cell death or rate of migration (Person et al., 2005b). Measures of phospho-histone H3 expression, TUNEL-positive cells and cell migration suggest that these alternative mechanisms are unlikely. Together, the data argue that OLFM1 regulates mesenchymal cell numbers by altering EMT. The morphology of activated endothelial cells after anti-OLF1 treatment suggests that OLFM1 acts late in EMT. Observations of marker gene regulation reinforce this idea. An early element of EMT is a loss of cell-cell adhesion (Nieto, 2011). OLFM1 does not induce a loss of adhesion molecule transcription. The effect of anti-OLF1 on cadherin5 and PECAM transcripts may reflect a re-epithelialization of activated endothelium rather than invasion.

Mesenchymal cells in the heart express both *FBLN2* and *POSTN* (Rongish et al., 1998; Kruzyńska-Frejtag et al., 2001). Exogenous OLFM1 up-regulates mRNA for both markers while the antibody inhibits their expression. Similarly, the markers *FLT1*, *FLK1* and *ALDH1A1* changed in a manner consistent with mesenchymal cell differentiation or invasion. Unlike the secreted molecules *POSTN* and *FBLN2*, *FLK1* and *ALDH1A1* were unaffected by the blocking antibody. We suggest that loss of expression of secreted markers is specific to mesenchymal cells while markers that remain unaffected by anti-OLFM1 are first expressed in the activated endothelial population, and therefore are unchanged by loss of OLFM1.

TGFβ isoforms are expressed in activated endothelia and newly formed mesenchymal cells as well as being expressed by the myocardium as an inductive signal (Potts and Runyan, 1989; Barnett et al., 1994; Boyer et al., 1999). Altered expression of TGFβ isoforms by both OLFM1 and anti-OLFM1 is consistent with formation of invasive mesenchyme. Expression of TGFβ3 by activated endothelia is auto-regulatory and provides an amplification of EMT (Ramsdell and Markwald, 1997). We found that OLFM1 is similarly auto-regulatory in cardiac explants and in MDCK cells. Auto-regulation of *OLFM1* by OLFM1 was also observed in a mouse cardiac mesenchymal cell line and in human glioblastoma cells (unpublished data). Auto-regulation by both TGFβ and OLFM1 may be a useful mechanism to ensure that EMT proceeds to completion. Despite the activities of these two ligands, the majority of endothelial cells do not complete invasion, but revert to differentiated endothelia. This suggests that there are either strong inhibitory signals that prevent completion of EMT or that only a subset of activated endothelial cells receive adequate signals to complete invasion. Our dose response curve showed that higher levels of OLFM1 inhibited mesenchymal marker expression in the heart. This suggests that OLFM1 may be both stimulatory and inhibitory of EMT. Strikingly, higher levels of OLFM1 had no such inhibitory effect on MDCK cells. The basis for this difference is not understood but may be exploited in the future to understand signal transduction in response to OLFM1.

The observation that MDCK epithelial cells respond to OLFM1, and more strongly to the combination of OLFM1 and TGFβ2, suggests that OLFM1 activity in relation to cell invasion is not unique to the chick. As TGFβ isoforms are endogenous in heart tissue, MDCK culture provided an opportunity to explore OLFM1 activity with or without TGFβ. OLFM1 has been knocked out in the mouse (Cheng et al., 2007) but the heart phenotype was not examined. As there are 4 OLFM genes and another 4 OLFM-related genes, there is potential redundancy that would obscure the role of OLFM1 in developmental EMTs (Tomarev and Nakaya, 2009). The receptor for OLFM1 has not yet been identified. OLFM4 is a related but distinct gene product associated with metastasis (Grover et al., 2010). Its olfactomedin domain is thought to bind to cells via *n*-acetylglucosamine residues and cell surface lectins (Grover et al., 2010). Whether the two different OLFMs act similarly is unclear but EMT could be related to both proteins and they may have similar receptor mechanisms.

In summary, these results show that OLFM1 is a novel mediator of invasion during EMT in the heart. It is co-expressed with TGF-β3, another mediator of cell invasion (Boyer et al., 1999), and appears to regulate a subset of EMT markers, especially proteases and secreted products. Morphology of the endothelia and the expression of EMT markers points most directly to a role in the conversion of activated endothelia to invasive mesenchyme. We show that this conversion of the activated epithelial cells into invasive mesenchyme is a specific regulated step that can be seen as a checkpoint in EMT progression. In the absence of the signaling required to pass the checkpoint, cells undergoing EMT may either revert to an epithelial phenotype or remain in a poorly invasive metastable state (Klymkowsky and Savagner, 2009). In development, both neural crest and valve progenitors appear to use TGFβ and OLFM1 (Duband et al., 1995; Boyer et al., 1999;

Barembaum et al., 2000). As OLFM1 is a conserved molecule across species, the concept of an invasion checkpoint has implications in adult pathology. Cancer metastasis and organ fibrosis both utilize EMT programs to invade surrounding tissue (Kallergi et al., 2011; Wang et al., 2011; Zhang et al., 2011). Demonstration that MDCK cells respond to OLFM1 in an invasion assay suggests that this checkpoint function is not restricted to the avian embryo. The data demonstrate a synergy between TGFβ and OLFM1 seen in both chick embryo tissue and MDCK cells. We expect OLFM1 to have a similar role in other EMTs. A survey of the Oncomine and GEO databases shows that OLFM1 is up-regulated in a number of cancers (Sun et al., 2006; Kim et al., 2010). OLFM1 expression may have a direct relationship to the aggressiveness of specific tumors. Thus, the role of this molecule in human EMT pathology may be as important as in development.

METHODS:

Chicken Embryo Isolation

Fertilized White Leghorn chicken eggs were obtained from MacIntire Eggs (San Diego, CA). Eggs were incubated at 37° C for 48-54 hours to obtain embryos at Hamburger and Hamilton stage 15. Using a dissecting stereo microscope, embryos were dissected free of embryonic membranes in 4°C sterile 1X Tyrode's salt buffer. Embryos were then rinsed in fresh sterile Tyrode's buffer to dissect out the AV canal segment of the heart with #5 forceps. A video showing the dissection and subsequent assay is available from the corresponding author upon request.

Collagen Gel Invasion Assay

Collagen gels were prepared as previously described (Potts et al., 1992; Boyer et al., 1999). OLFM1 (#4636-NL) and anti-OLFM1 (#AF4636) were obtained from R&D systems (Minneapolis, MN). AV canal explants were treated with OLFM1 (100-400 ng/μL) or antibody (10 μg/ml) to determine the effects on EMT and molecular regulators of EMT. After treatment, AV canal explants were incubated on the collagen gel for 36 hours. One set of explants was collected and fixed in 4% paraformaldehyde (PFA) for 30 minutes. Cell counts and micrographs were taken to identify morphological differences between treated and untreated cultures. Explants were observed on an inverted microscope equipped with Hoffman Modulation Optics to collect mesenchymal cell counts or prepared for cell proliferation assays. Mesenchymal cells were blindly counted by different lab members to prevent any bias. Additional explants were extracted to collect mRNA for real time RT-PCR. Some explants were prepared for TUNEL assay (below) or phospho-H3 histone staining (Sigma-Aldrich, St. Louis, MO # H0412).

Collagen Gel Migration Assay

Stage 15 AV canal explants were placed on collagen gels and incubated overnight with 5% CO₂ at 37 °C (18 hours). Explants were then treated with OLFM1 (200 ng/mL) for 4 hours. The 4-hour treatment was selected as auto-regulatory expression of OLFM1 can be seen at this time. The interval is consistent with migration assays investigating the effects of HGF on cell migration (Takeuchi et al., 1996). After a 4-hour exposure, explant images were obtained for 3 hr using time lapse capture on an Olympus (IMT-2) microscope equipped with Hoffman Modulation Optics. Time-lapse images were captured every three minutes. To measure mesenchymal cell migration tracks, a centroid was assigned to each cell image and Simple PCI software was used to accumulate the movement over 3 hr. A total of twenty cells were measured for each control and OLFM1 treatment.

OLFM1 siRNA Treatment of AV canals

Silencer® Select Custom Designed siRNA for OLFM1 was obtained from Ambion (#s444361). The siRNA was suspended and diluted in nuclease free water to obtain a working solution of 500 nM. AV canal were explanted as previously described in the Embryo Isolation Section and placed in 500 μL of 1XM199 (working solution). The working solution contained a final siRNA concentration of 5 nM. To facilitate entry of

siRNA oligos into the cell 5 μ L of siPORT™ NeoFX™ (cat) transfecting agent was added to the working solution. The AV canals were incubated in siRNA working solution at 37°C and 5% CO₂ for 45 minutes. These conditions were used as they were optimized in previous published work (Mercado-Pimentel et al., 2007; Tavares et al., 2007). After incubation AV canals were placed on collagen gels to allow EMT and mesenchymal cell migration. The number of invaded cells were counted and compared to a scrambled control. The scrambled control used is a 21 oligonucleotide template that did not blast to any gene in the chicken genome, 5'-AGACTGTCGCTGCTGTCC-3'. The siRNA target sequence for the OLFM1 was 5'-GCAUAGACCUGACAGAUCAtt-3', which targets the olfactomedin domain of the molecule.

Immunofluorescent Microscopy

Embryos were collected and rinsed in Tyrode's solution. Embryos were cryofixed by protocol after Kitten et al., (1987). Briefly, embryos were flash frozen by dropping them into N-butanol in vials suspended in liquid nitrogen. The N-butanol was kept above freezing by inserting a metal rod at intervals. Frozen embryos were removed with forceps (at liquid nitrogen temperature) and placed in a scintillation vial containing Molecular Sieve beads and frozen 100% ethanol with an overlying layer of liquid nitrogen. The vials were capped loosely and placed in a -80°C freezer for 3-5 days. Subsequently the embryos were rinsed in 100% ethanol at -20°C and shifted into 100% Xylene and embedded in paraffin. Paraffin blocks were sectioned and the sections affixed to glass slides. Slides were de-paraffinized in Xylene, hydrated in an ethanol series from 100% ethanol to 100% phosphate buffered saline (PBS). Sections were rinsed in PBS for 10 minutes, and blocked for 1 hour at room temperature. Blocking solution contained 1% BSA and 0.1% Tween 20 suspended in PBS. Sections containing AV canal and heart tissue were incubated overnight with primary antibody at 4 °C in a humid chamber. Slides were rinsed with 1X PBS, three times, and Cys™ rabbit anti-sheep IgG was used as a secondary antibody (KPL, Gaithersburg MD, # 072-02-23-06) in a humid chamber for 2 hours at room temperature. The slides were then exposed to DAPI (Sigma-Aldrich, St. Louis, MO #. D8417) as a counter stain for nuclei. Vectashield was used as a mounting media (Vector Laboratories, Burlingame, CA, # H-1000) to prevent loss of fluorescent signal. Samples were then examined using a Delta-Vision Olympus IX 70 microscope.

TUNEL Assay

Damaged and fragmented DNA was detected by TdT (terminal deoxynucleotidyl transferase)-mediated dUTP nick-end labeling (TUNEL) assay using the DeadEnd Fluorometric TUNEL System kit (Promega, Madison, WI, #G3250). Explants on collagen gels were treated with 10 μ g/ml anti-OLFM1 antibody for 36 hours. The explants were fixed with 4% paraformaldehyde and permeabilized with 0.1% Triton X-100. Tissues were labeled by incubation in 50 μ L TUNEL reaction mixture containing the mixture of terminal deoxynucleotidyl transferase at dUTP. The labeling of AV explants was done in the dark at 37°C for 1 hour. Cellular nuclei were stained using DAPI 1:10000 (Sigma, MO) fluorescent stain. AV canal explants (n=20) for control and treated including endothelial outgrowth were randomly selected for analysis. Approximately 100 cells were counted from each explant. Analysis was performed using a fluorescent microscope and cells were categorized as apoptotic (green nuclear fluorescence) or normal (no fluorescence). Samples were analyzed using a Delta-Vision Olympus IX 70 microscope.

Proliferation/Immunostaining Assay

Proliferating cells were detected by immunostaining for phospho-Histone H3 (ser 10). The collagen gels with cultured AV explants were treated with OLFM1 (200 ng/mL) for 36 hours. The AV explants were then fixed in 4% paraformaldehyde and permeabilized with 0.1% Triton X. Polyclonal rabbit antibody for phospho-histone H3 was used as the primary antibody at a 1:300 dilution (Sigma-Aldrich, St. Louis, MO, # Ho412). After washing with 1X PBS, Alexa 546 goat anti-rabbit IgG in a 1:400 dilution was used as the secondary antibody (Molecular

Probes, CA). 1X PBS was used to wash excess secondary antibody and DAPI 1:10000 (Sigma, St. Louis, MO) was used to counter stain cell nuclei. AV canal explants (n=20) from control and treated including epithelial outgrow were randomly selected for analysis and approximately 100 cells were counted from each explant. Analysis was performed using a fluorescent microscope and cells were categorized as either proliferating (red nuclear fluorescence) or normal (no red fluorescence). Samples were then analyzed using a Delta-Vision Olympus IX 70 microscope.

Western Blotting

Heads and hearts from stage 17 chicken embryos were collected to obtain a whole-cell lysate using NP-40 buffer (20 mM Tris-HCL, 137 mM NaCl, 10% glycerol, 1% Nonidet P-40, 2 mM EDTA) at 4°C. The lysis NP-40 buffer was supplemented with a Proteinase inhibitor cocktail table (Roche, IN) every time before use. Cell lysates were also sonicated for 20 seconds and the protein concentration was determined using Pierce 660 nm Protein Assay (Thermo Scientific, IL). Equal amounts of head and heart (28 μ g) samples were loaded on a 10% acrylamide gel. Protein was then transferred to nitrocellulose membrane using the Trans-Blot Turbo System (Bio-rad, CA). OLFM1 protein was detected using Anti-mouse Noelin-1 Antibody (R&D Systems, MN) as a primary antibody in 1:400 dilution (0.25 μ g/mL) overnight at 4°C. The corresponding secondary antibody was used in 1:10,000 dilution at room temperature for 2 hours. Bands were then visualized using the Li-Cor Odyssey infrared imaging system.

Trans-well Invasion Assay

Madin-Darby Canine Kidney Epithelial (MDCK) Cells (50,000/well) were plated onto Trans-well culture dishes (8 μ m pore size, BD Falcon, NJ) containing 100 μ L of solidified Matrigel™ Matrix (Bioscience, MA). Cells were treated 200 ng/mL OLFM1 alone, 2 ng/mL of TGF β 2 or a combination of both factors for 24 hours. The membranes were removed from the culture inserts, inverted to display the lower surface and with crystal violet stain. Cells that traversed the matrix and membrane were counted and total numbers for each membrane were compared to untreated controls.

Quantitative Real-Time RT-PCR

Total RNA was extracted from AV canal explants cultured on the collagen gel by using TRIZOL reagent (Gibco BRL). RNA was DNase treated with TURBO-DNA free kit (Ambion). cDNA was transcribed using the iScript cDNA synthesis kit (Bio-Rad, Richmond, CA). Data normalization against the specific housekeeping genes (GAPDH, LDH, β -actin, and mitochondrial DNA) was problematic due to either the substantial phenotypic change during EMT or to the effects of the treatment. Therefore, total cDNA was used to normalize the quantitative PCR reactions. To sensitively measure cDNA in each reaction, Quanti-iT Oligreen ssDNA reagent (Molecular Probes, CA) was used to measure and aliquot single-stranded cDNA in combination with a fluorometer (Turner Biosystems). Names, UID, numerical data and significance are shown in Supplemental Table 1. Primer sequences for the selected genes are listed in Supplemental table 2.

Statistics

All comparisons employed Student's T-test (paired, 2 tailed) with a $p \leq 0.05$ with a control group. The mesenchymal cell numbers counted in figure 3 included an N of 20 explants in each group. Proliferating and apoptotic cells (fig. 4a-b) also include an N of 20 explants for each treatment. Track length measurements (fig. 4c) were performed with tracks of 20 cells for treated and control samples. All real time RT-PCR data is presented as a measure of 3, independently collected, pools of 15-20 AV canal explants. Data from each pooled sample is averaged from 2 or 3 technical repeats. Names, UID, numerical data and significance are shown in Supplemental Table 2.

Picture Processing

Adobe Photoshop CS4 Version 11.0.2 software was used to handle and process pictures. The picture processing included changes in: Brightness/contrast and re-sizing in order to clearly evaluate samples and easily determine differences from control. Picture processing was performed identically on all micrographs in each comparison.

ACKNOWLEDGEMENTS:

We would like to thank Drs. Moran-Segura, Sourav Ghosh, Jean Wilson, Paul Krieg, Parker Antin and the Heart Development group at the University of Arizona for useful discussions. We thank Jade Rusche and Jessica Bender for technical support. Thanks also go to Laura Serrano, Michael J. Sullivan and Dr. Albert McHenry. We thank Tony Person for first drawing our attention to OLFM1. Research funding was from NIH HL82851 and a grant from the University of Arizona Sarver Heart Center. Student support was from MGE@MSA - AGEP (NSF) Cooperative Agreement No. HRD-0450137 and NIH T32 ES007091. Research resources (imaging) were supported by NIH ES006694. In situ hybridization performed for this study by the Geisha Project was supported by NIH P41HDO64559.

Competing Interests

There are no current financial or competing interests on the part of any of the authors. The authors have filed a disclosure to the University of Arizona for a preliminary patent on OLFM1 as a potential target to inhibit cell invasion in metastasis or organ fibrosis.

Author Contributions

This work was performed largely as thesis research by Alejandro Lencinas and he wrote the first draft of the manuscript. Danny Chhun, Kelvin Dan and Kristen Ross contributed data from their work with MDCK cells and specific markers of EMT. Elizabeth Hoover provided data from her examination of ALDH1a1. Parker Antin provided data from in situ examination of OLFM1 family members in the developing chick. Raymond Runyan directed the research, integrated the components of the project and wrote the final version of the manuscript.

Translational Impact

Epithelial-mesenchymal transition (EMT) is a cellular process widely used by the embryo to generate three-dimensional structure. In the adult, EMT is largely a pathological process associated with metastasis and organ fibrosis. The EMT that forms the valvular progenitors of the heart is a prototypical EMT that first defined the process as being regulated by tissue interaction and subsequently by TGFβ and its receptors. Though there is considerable interest in targeting TGFβ as a mediator of pathological EMT, its concurrent regulation of immune responses presents a complication. This report strengthens the identification of EMT as a multistep process and identifies a novel component of EMT, OLFM1, which could be targeted to prevent secondary metastases and reduce organ fibrosis. Observations that it is synergistic with TGFβ and that it is auto-regulatory provide novel perspectives on EMT.

REFERENCES:

- Barembaum, M., Moreno, T. A., LaBonne, C., Sechrist, J. and Bronner-Fraser, M. (2000) 'Noelin-1 is a secreted glycoprotein involved in generation of the neural crest.', *Nature Cell Biology* 2(4): 219-225.
- Barnett, J. V. and Desgrosellier, J. S. (2003) 'Early events in valvulogenesis: a signaling perspective', *Birth Defects Res Part C Embryo Today* 69(1): 58-72.
- Barnett, J. V., Moustakas, A., Lin, W., Wang, X. F., Lin, H. Y., Galper, J. B. and Maas, R. L. (1994) 'Cloning and developmental expression of the chick type II and type III TGFβ receptors', *Developmental Dynamics* 199: 12-27.
- Boyer, A. S., Ayerinkas, II, Vincent, E. B., McKinney, L. A., Weeks, D. L. and Runyan, R. B. (1999) 'TGF beta 2 and TGF beta 3 have separate and sequential activities during epithelial-mesenchymal cell transformation in the embryonic heart', *Developmental Biology* 208(2): 530-545.
- Brown, C. B., Boyer, A. S., Runyan, R. B. and Barnett, J. V. (1996) 'Antibodies to the type II TGF beta receptor block cell activation and migration during atrioventricular cushion transformation in the heart', *Developmental Biology* 174(2): 248-257.
- Camenisch, T. D., Molin, D. G. M., Person, A., Runyan, R. B., Gittenberger-de Groot, A. C., McDonald, J. A. and Klewer, S. E. (2002) 'Temporal and distinct TGF beta ligand requirements during mouse and avian endocardial cushion morphogenesis', *Developmental Biology* 248(1): 170-181.
- Comijn, J., Berx, G., Vermassen, P., Verschuere, K., van Grunsven, L., Bruyneel, E., Mareel, M., Huylebroeck, D. and van Roy, F. (2001) 'The two-handed E box binding zinc finger protein SIP1 downregulates E-cadherin and induces invasion', *Molecular Cell* 7(6): 1267-1278.
- Derynck, R. and Akhurst, R. J. (2007) 'Differentiation plasticity regulated by TGF-beta family proteins in development and disease', *Nature Cell Biology* 9(9): 1000-4.
- Duband, J. L., Monier, F., Delannet, M. and Newgreen, D. (1995) 'Epithelium-mesenchyme transition during neural crest development', *Acta Anatomica* 154(1): 63-78.
- Ginestier, C., Hur, M. H., Charafe-Jauffret, E., Monville, F., Dutcher, J., Brown, M., Jacquemier, J., Viens, P., Kleer, C. G., Liu, S. et al. (2007) 'ALDH1 is a marker of normal and malignant human mammary stem cells and a predictor of poor clinical outcome', *Cell Stem Cell* 1(5): 555-67.
- Grover, P. K., Hardingham, J. E. and Cummins, A. G. (2010) 'Stem cell marker olfactomedin 4: critical appraisal of its characteristics and role in tumorigenesis', *Cancer and metastasis reviews* 29(4): 761-75.
- Hamburger, V. and Hamilton, H. L. (1951) 'A series of normal stages in the development of the chick embryo', *Journal of Morphology* 88: 49-92.
- Hay, E. D. (1995) 'An overview of epithelio-mesenchymal transformation', *Acta Anatomica* 154(1): 8-20.
- Kallergi, G., Papadaki, M., Politaki, E., Mavroudis, D., Georgoulas, V. and Agelaki, S. (2011) 'Epithelial to mesenchymal transition markers expressed in circulating tumour cells of early and metastatic breast cancer patients', *Breast Cancer Research* 13(3): R59.
- Kessenbrock, K., Plaks, V. and Werb, Z. (2010) 'Matrix metalloproteinases: regulators of the tumor microenvironment', *Cell* 141(1): 52-67.
- Kim, S. M., Park, Y. Y., Park, E. S., Cho, J. Y., Izzo, J. G., Zhang, D., Kim, S. B., Lee, J. H., Bhutani, M. S., Swisher, S. G. et al. (2010) 'Prognostic biomarkers for esophageal adenocarcinoma identified by analysis of tumor transcriptome', *Public Library of Science one* 5(11): e15074.
- Kitten, G. T., Markwald, R. R. and Bolender, D. L. (1987) 'Distribution of basement membrane antigens in cryopreserved early embryonic hearts', *Anatomical Record* 217(4): 379-390.
- Klymkowsky, M. W. and Savagner, P. (2009) 'Epithelial-mesenchymal transition: a cancer researcher's conceptual friend and foe.', *Am J Pathology* 174(5): 1588-93.
- Krug, E. L., Runyan, R. B. and Markwald, R. R. (1985) 'Protein extracts from early embryonic hearts initiate cardiac endothelial cytodifferentiation', *Developmental Biology* 112(2): 414-426.
- Kruzynska-Frejtak, A., Machnicki, M., Rogers, R., Markwald, R. R. and Conway, S. J. (2001) 'Periostin (an osteoblast-specific factor) is expressed within the embryonic mouse heart during valve formation', *Mechanisms of Development* 103(1-2): 183-8.
- Lincoln J, K. R., Scherer G, Yutzey KE. (2007) 'Sox9 is required for precursor cell expansion and extracellular matrix organization during mouse heart valve development.', *Dev Biol.* 305(1): 120-32.
- Markwald, R. R., Fitzharris, T. P. and Manasek, F. J. (1977) 'Structural Development Of Endocardial Cushions', *American Journal Of Anatomy* 148(1): 85-119.
- Markwald, R. R., Runyan, R. B., Kitten, G. T., Funderburg, F. M., Bernanke, D. H. and Brauer, P. R. (1984) 'Use of collagen gel cultures to study heart development: proteoglycan and glycoprotein interactions during formation of endocardial cushion tissue. in R. L. Treilstad (ed.) The Role of Extracellular Matrix in Development. New York: Alan R. Liss, Inc.
- Mercado-Pimentel, M. E., Hubbard, A. D. and Runyan, R. B. (2007) 'Endoglin and Alk5 regulate epithelial-mesenchymal transformation during cardiac valve formation', *Developmental Biology* 304(1): 420-432.
- Moreno, T. A. and Bronner-Fraser, M. (2002) 'Neural expression of mouse Noelin-1/2 and comparison with other vertebrates.', *Mechanisms of Development* 119(1): 121-5.
- Moreno, T. A. and Bronner-Fraser, M. (2005) 'Noelins modulate the timing of neuronal differentiation during development', *Developmental Biology* 288(2): 434-47.
- Nieto, M. A. (2011) 'The ins and outs of the epithelial to mesenchymal transition in health and disease', *Annual review of cell and developmental biology* 10(27): 347-76.
- Nieto, M. A., Sargent, M. G., Wilkinson, D. G. and Cooke, J. (1994) 'Control of Cell Behavior During Vertebrate Development by Slug, a Zinc Finger Gene.', *Science* 264: 835-839.
- Peinado, H., Olmeda, D. and Cano, A. (2007) 'Snail, Zeb and bHLH factors in tumour progression: an alliance against the epithelial phenotype?', *Nature reviews. Cancer* 7(6): 415-28.

30. Person, A. D., Garriock, R. J., Krieg, P. A., Runyan, R. B. and Klewer, S. E. (2005a) 'Frzb modulates Wnt-9a-mediated beta-catenin signaling during avian atrioventricular cardiac cushion development', *Developmental Biology* 278(1): 35-48.
31. Person, A. D., Klewer, S. E. and Runyan, R. B. (2005b) 'Cell Biology of Cardiac Cushion Development', *International Review of Cytology* 243: 287-335.
32. Potts, J. D. and Runyan, R. B. (1989) 'Epithelial-mesenchymal cell transformation in the embryonic heart can be mediated, in part, by transforming growth factor β ', *Developmental Biology* 134(2): 392-401.
33. Potts, J. D., Vincent, E. B., Runyan, R. B. and Weeks, D. L. (1992) 'Sense and antisense TGF beta 3 mRNA levels correlate with cardiac valve induction', *Developmental Dynamics* 193(4): 340-345.
34. Ramsdell, A. F. and Markwald, R. R. (1997) 'Induction of endocardial cushion tissue in the avian heart is regulated, in part, by TGFbeta-3-mediated autocrine signaling', *Developmental Biology* 188(1): 64-74.
35. Romano, L. A. and Runyan, R. B. (1999) 'Slug is a mediator of epithelial-mesenchymal cell transformation in the developing chicken heart', *Developmental Biology* 212(1): 243-254.
36. Rongish, B. J., Drake, C. J., Argraves, W. S. and Little, C. D. (1998) 'Identification of the developmental marker, JB3-antigen, as fibrillin-2 and its de novo organization into embryonic microfibrillar arrays', *Dev Dyn* 212(3): 461-71.
37. Runyan, R. B. and Markwald, R. R. (1983) 'Invasion of mesenchyme into three-dimensional collagen gels: A regional and temporal analysis of interaction in embryonic heart tissue.', *Developmental Biology* 95: 108-114.
38. Runyan, R. B., Potts, J. D., Sharma, R. V., Loeber, C. P., Chiang, J. J. and Bhalla, R. C. (1990) 'Signal Transduction of a Tissue Interaction During Embryonic Heart Development', *Cell Regulation* 1(3): 301-313.
39. Stankunas, K., Ma, G. K., Kuhnert, F. J., Kuo, C. J. and Chang, C. P. (2010) 'VEGF signaling has distinct spatiotemporal roles during heart valve development', *Developmental Biology* 347(2): 325-36.
40. Sun, L. C., Hui, A. M., Su, Q., Vortmeyer, A., Kotliarov, Y., Pastorino, S., Passaniti, A., Menon, J., Walling, J., Bailey, R. et al. (2006) 'Neuronal and glioma-derived stem cell factor induces angiogenesis within the brain', *Cancer Cell* 9(4): 287-300.
41. Takeuchi, K., Shibamoto, S., Hayakawa, M., Hori, T., Miyazawa, K., Kitamura, N. and ITO, F. (1996) 'Hepatocyte Growth Factor (HGF)-Induced Cell Migration Is Negatively Modulated by Epidermal Growth Factor through Tyrosine Phosphorylation of the HGF Receptor', *Experimental Cell Research* (223): 420-425.
42. Tavares, A. L., Mercado-Pimentel, M. E., Runyan, R. B. and Kitten, G. T. (2007) 'TGF beta-mediated RhoA expression is necessary for epithelial-mesenchymal transition in the embryonic chick heart', *Development Dynamics* 235(6): 1589-98.
43. Tavares, A. L. P., Mercado-Pimentel, M.E., Runyan, R.B., Kitten, G. T. (2006) 'TGF-mediated RhoA expression is necessary for epithelial-mesenchymal transition in the embryonic chick heart', *Developmental Dynamics* 235(6): 1589-1598.
44. Thiery, J. P., Acloque, H., Huang, R. Y. and Nieto, M. A. (2009) 'Epithelial-mesenchymal transitions in development and disease', *Cell* 139(5): 871-90.
45. Tomarev, S. I. and Nakaya, N. (2009) 'Olfactomedin Domain-Containing Proteins: Possible Mechanisms of Action and Functions in Normal Development and Pathology', *Molecular Neurobiology* (40): 122-138.
46. Van de Putte, T., Maruhashi, M., Francis, A., Nelles, L., Kondoh, H., Huylebroeck, D. and Higashi, Y. (2003) 'Mice lacking ZFHx1B, the gene that codes for Smad-interacting protein-1, reveal a role for multiple neural crest cell defects in the etiology of Hirschsprung disease-mental retardation syndrome.', *American Journal of Human Genetics* 72(2): 465-70.
47. Wang, X., Lu, H., Urvalek, A. M., Li, T., Yu, L., Lamar, J., DiPersio, C. M., Feustel, P. J. and Zhao, J. (2011) 'KLF8 promotes human breast cancer cell invasion and metastasis by transcriptional activation of MMP9', *Oncogene* 30(16): 1901-11.
48. Wunsch, A. M., Little, C. D. and Markwald, R. R. (1994) 'Cardiac endothelial heterogeneity defines valvular development as demonstrated by the diverse expression of JB3, an antigen of the endocardial cushion tissue', *Developmental Biology (Orlando)* 165(2): 585-601.
49. Yang, J. and Weinberg, R. A. (2008) 'Epithelial-mesenchymal transition: at the crossroads of development and tumor metastasis.', *Developmental Cell* 14(6): 818-29.
50. Yeh, M. W., Rougier, J. P., Park, J. W., Duh, Q. Y., Wong, M., Werb, Z. and Clark, O. H. (2006) 'Differentiated thyroid cancer cell invasion is regulated through epidermal growth factor receptor-dependent activation of matrix metalloproteinase (MMP)-2/gelatinase A.', *Endocrine-related cancer* 13(4): 1173-83.
51. Zhang, H. J., Wang, H. Y., Zhang, H. T., Su, J. M., Zhu, J., Wang, H. B., Zhou, W. Y., Zhang, H., Zhao, M. C., Zhang, L. et al. (2011) 'Transforming growth factor- β 1 promotes lung adenocarcinoma invasion and metastasis by epithelial-to-mesenchymal transition.', *Molecular and cellular biochemistry* 355(1-2): 309-14.
52. Wang, X., Lu, H., Urvalek, A.M. Li, T., Yu, L., Lamar, J., DiPersio, C.M., Feustel, P.J. and Zhao, J. (2011) KLF8 promotes human breast cancer cell invasion and metastasis by transcriptional activation of MMP9. *Oncogene* 30, 1901-1911 mesenchymal cell numbers ($p > 0.05$) and the combination reduced mesenchymal numbers still further ($p > 0.001$)